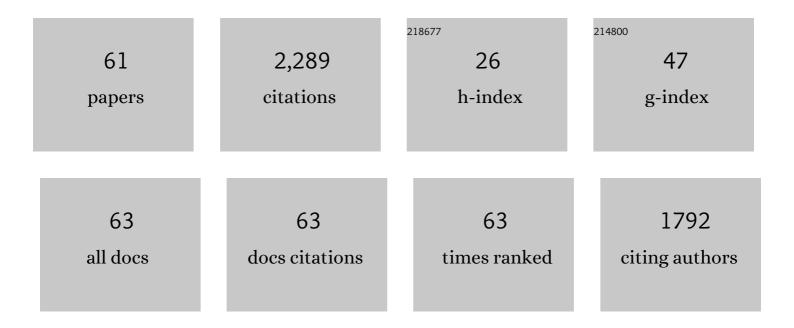
Wei-qiang Li

List of Publications by Year in descending order

Source: https://exaly.com/author-pdf/8449133/publications.pdf Version: 2024-02-01



WELOWNELL

#	Article	IF	CITATIONS
1	Biological Fe oxidation controlled deposition of banded iron formation in the ca. 3770Ma Isua Supracrustal Belt (West Greenland). Earth and Planetary Science Letters, 2013, 363, 192-203.	4.4	146
2	Magnesium isotope fractionation during precipitation of inorganic calcite under laboratory conditions. Earth and Planetary Science Letters, 2012, 333-334, 304-316.	4.4	127
3	Biologically recycled continental iron is a major component in banded iron formations. Proceedings of the National Academy of Sciences of the United States of America, 2015, 112, 8193-8198.	7.1	121
4	The Cu isotopic signature of granites from the Lachlan Fold Belt, SE Australia. Chemical Geology, 2009, 258, 38-49.	3.3	115
5	Experimental calibration of Mg isotope fractionation between dolomite and aqueous solution and its geological implications. Geochimica Et Cosmochimica Acta, 2015, 157, 164-181.	3.9	115
6	A redox-stratified ocean 3.2 billion years ago. Earth and Planetary Science Letters, 2015, 430, 43-53.	4.4	114
7	Copper isotopic zonation in the Northparkes porphyry Cu–Au deposit, SE Australia. Geochimica Et Cosmochimica Acta, 2010, 74, 4078-4096.	3.9	106
8	Precise measurement of stable potassium isotope ratios using a single focusing collision cell multi-collector ICP-MS. Journal of Analytical Atomic Spectrometry, 2016, 31, 1023-1029.	3.0	104
9	K isotopes as a tracer for continental weathering and geological K cycling. Proceedings of the National Academy of Sciences of the United States of America, 2019, 116, 8740-8745.	7.1	99
10	Magnesium isotope fractionation between brucite [Mg(OH)2] and Mg aqueous species: Implications for silicate weathering and biogeochemical processes. Earth and Planetary Science Letters, 2014, 394, 82-93.	4.4	84
11	An anoxic, Fe(II)-rich, U-poor ocean 3.46 billion years ago. Geochimica Et Cosmochimica Acta, 2013, 120, 65-79.	3.9	76
12	Exchange and fractionation of Mg isotopes between epsomite and saturated MgSO4 solution. Geochimica Et Cosmochimica Acta, 2011, 75, 1814-1828.	3.9	64
13	Felsic volcanism as a factor driving the end-Permian mass extinction. Science Advances, 2021, 7, eabh1390.	10.3	63
14	Contrasting behavior of oxygen and iron isotopes in banded iron formations revealed by in situ isotopic analysis. Earth and Planetary Science Letters, 2013, 384, 132-143.	4.4	53
15	Origin of heavy Fe isotope compositions in high-silica igneous rocks: A rhyolite perspective. Geochimica Et Cosmochimica Acta, 2017, 218, 58-72.	3.9	50
16	Potassium isotopic composition of various samples using a dual-path collision cell-capable multiple-collector inductively coupled plasma mass spectrometer, Nu instruments Sapphire. Chemical Geology, 2021, 571, 120144.	3.3	49
17	Atom Exchange between Aqueous Fe(II) and Structural Fe in Clay Minerals. Environmental Science & Technology, 2015, 49, 2786-2795.	10.0	46
18	Resetting of Mg isotopes between calcite and dolomite during burial metamorphism: Outlook of Mg isotopes as geothermometer and seawater proxy. Geochimica Et Cosmochimica Acta, 2017, 208, 24-40.	3.9	45

Wei-qiang Li

#	Article	IF	CITATIONS
19	Zinc Isotope Fractionation during Sorption onto Al Oxides: Atomic Level Understanding from EXAFS. Environmental Science & Technology, 2018, 52, 9087-9096.	10.0	40
20	Potassium isotope fractionation between K-salts and saturated aqueous solutions at room temperature: Laboratory experiments and theoretical calculations. Geochimica Et Cosmochimica Acta, 2017, 214, 1-13.	3.9	38
21	Environmental applications of metal stable isotopes: Silver, mercury and zinc. Environmental Pollution, 2019, 252, 1344-1356.	7.5	36
22	Mg isotope response to dolomitization in hinterland-attached carbonate platforms: Outlook of Î′26Mg as a tracer of basin restriction and seawater Mg/Ca ratio. Geochimica Et Cosmochimica Acta, 2018, 235, 189-207.	3.9	35
23	Iron Isotope Fractionations Reveal a Finite Bioavailable Fe Pool for Structural Fe(III) Reduction in Nontronite. Environmental Science & Technology, 2016, 50, 8661-8669.	10.0	31
24	Vital effects of K isotope fractionation in organisms: observations and a hypothesis. Acta Geochimica, 2017, 36, 374-378.	1.7	30
25	Conservative behavior of Mg isotopes in massive dolostones: From diagenesis to hydrothermal reworking. Sedimentary Geology, 2019, 381, 65-75.	2.1	30
26	Geochemistry and cosmochemistry of potassium stable isotopes. Chemie Der Erde, 2021, 81, 125786.	2.0	30
27	Updating the Geologic Barcodes for South China: Discovery of Late Archean Banded Iron Formations in the Yangtze Craton. Scientific Reports, 2017, 7, 15082.	3.3	27
28	Effects of early diagenesis on Mg isotopes in dolomite: The roles of Mn(IV)-reduction and recrystallization. Geochimica Et Cosmochimica Acta, 2019, 250, 1-17.	3.9	24
29	Iron isotope fractionation in sediments of an oligotrophic freshwater lake. Earth and Planetary Science Letters, 2015, 423, 164-172.	4.4	23
30	Subglacial meltwater supported aerobic marine habitats during Snowball Earth. Proceedings of the National Academy of Sciences of the United States of America, 2019, 116, 25478-25483.	7.1	23
31	Sn(II) chloride speciation and equilibrium Sn isotope fractionation under hydrothermal conditions: A first principles study. Geochimica Et Cosmochimica Acta, 2021, 300, 25-43.	3.9	23
32	Existing forms of REE in gold-bearing pyrite of the Jinshan gold deposit, Jiangxi Province, China. Journal of Rare Earths, 2009, 27, 1079-1087.	4.8	21
33	Calibrating equilibrium Fe isotope fractionation factors between magnetite, garnet, amphibole, and biotite. Geochimica Et Cosmochimica Acta, 2020, 271, 78-95.	3.9	20
34	Alkylamine screening and zinc doping of highly luminescent 2D tin-halide perovskites for LED lighting. Materials Advances, 2021, 2, 1320-1327.	5.4	20
35	Geological cycling of potassium and the K isotopic response: insights from loess and shales. Acta Geochimica, 2019, 38, 508-516.	1.7	19
36	U–Th–Pb isotope data indicate phanerozoic age for oxidation of the 3.4Ga Apex Basalt. Earth and Planetary Science Letters, 2012, 319-320, 197-206.	4.4	18

Wei-qiang Li

#	Article	IF	CITATIONS
37	Sn isotope fractionation during volatilization of Sn(IV) chloride: Laboratory experiments and quantum mechanical calculations. Geochimica Et Cosmochimica Acta, 2020, 269, 184-202.	3.9	18
38	Precise measurement of ⁴¹ K/ ³⁹ K ratios by highâ€resolution multicollector inductively coupled plasma mass spectrometry under a dry and hot plasma setting. Rapid Communications in Mass Spectrometry, 2022, 36, e9289.	1.5	18
39	Mg isotope evidence for restriction events within the Paleotethys ocean around the Permian-Triassic transition. Earth and Planetary Science Letters, 2021, 556, 116704.	4.4	17
40	Extracting Mg isotope signatures of ancient seawater from marine halite: A reconnaissance. Chemical Geology, 2020, 552, 119768.	3.3	14
41	Termination of Cryogenian ironstone deposition by deep ocean euxinia. Geochemical Perspectives Letters, 0, 15, 1-5.	5.0	14
42	Transformation of amorphous precursor to crystalline carbonate: Insights from Mg isotopes in the dolomite-analogue mineral norsethite [BaMg(CO3)2]. Geochimica Et Cosmochimica Acta, 2020, 272, 1-20.	3.9	12
43	Formation mechanisms of hydrocarbon reservoirs associated with volcanic and subvolcanic intrusive rocks: Examples in Mesozoic-Cenozoic basins of eastern China. AAPG Bulletin, 2006, 90, 137-147.	1.5	11
44	On the coordination of Mg2+ in aragonite: Ab-initio absorption spectroscopy and isotope fractionation study. Geochimica Et Cosmochimica Acta, 2020, 286, 324-335.	3.9	11
45	Cu isotope systematics of conduit-type Cu–PGE mineralization in the Eastern Gabbro, Coldwell Complex, Canada. Mineralium Deposita, 2021, 56, 707-724.	4.1	11
46	Experimental investigation of the reactions between pyrite and aqueous Cu(I) chloride solution at 100–250†°C. Geochimica Et Cosmochimica Acta, 2021, 298, 1-20.	3.9	11
47	What drives Fe depletion in calc-alkaline magma differentiation: Insights from Fe isotopes. Geology, 2022, 50, 552-556.	4.4	10
48	Fingerprinting hydrothermal fluids in porphyry Cu deposits using K and Mg isotopes. Science China Earth Sciences, 2020, 63, 108-120.	5.2	9
49	The Neoproterozoic "Blood Falls―in Tarim Craton and Their Possible Connection With Snowball Earth. Journal of Geophysical Research F: Earth Surface, 2019, 124, 229-244.	2.8	8
50	Reactive iron isotope signatures of the East Asian dust particles: Implications for iron cycling in the deep North Pacific. Chemical Geology, 2020, 531, 119342.	3.3	8
51	Response of Mg isotopes to dolomitization during fluctuations in sea level: Constraints on the hydrological conditions of massive dolomitization systems. Sedimentary Geology, 2021, 420, 105922.	2.1	7
52	Iron isotope fractionation during sulfide liquid evolution in Cu–PGE mineralization of the Eastern Gabbro, Coldwell Complex, Canada. Chemical Geology, 2021, 576, 120282.	3.3	7
53	Recrystallization of dolostones in the Cambrian Xiaoerbrak Formation, Tarim Basin and possible link to reservoir development. Marine and Petroleum Geology, 2022, 136, 105452.	3.3	7
54	Reconstruct hydrological history of terrestrial saline lakes using Mg isotopes in halite: A case study of the Quaternary Dalangtan playa in Qaidam Basin, NW China. Palaeogeography, Palaeoclimatology, Palaeoecology, 2022, 587, 110804.	2.3	7

Wei-Qiang Li

#	Article	IF	CITATIONS
55	Accretion regions of meteorite parent bodies inferred from a two-endmember isotopic mixing model. Monthly Notices of the Royal Astronomical Society, 2022, 513, 363-373.	4.4	6
56	Isobaric Spike Method for Absolute Isotopic Ratio Determination by MC-ICP-MS. Analytical Chemistry, 2020, 92, 4820-4828.	6.5	5
57	Fe isotopic fractionation during the magmatic–hydrothermal stage of granitic magmatism. Lithos, 2019, 350-351, 105265.	1.4	4
58	Genesis of the Fulu Cryogenian iron formation in South China: Synglacial or interglacial?. Precambrian Research, 2022, 376, 106689.	2.7	4
59	Isotopic fingerprinting of dissolved iron sources in the deep western Pacific since the late Miocene. Science China Earth Sciences, 2020, 63, 1767-1779.	5.2	2
60	Dissolved Thorium Isotope Evidence for Export Productivity in the Subtropical North Pacific During the Late Quaternary. Geophysical Research Letters, 2020, 47, e2019GL085995.	4.0	2
61	Iron isotope constraints on the metal source and depositional environment of the Neoproterozoic banded iron- and manganese deposits in Urucum Brazil Chemie Der Erde 2021 81 125771	2.0	1